

## SEISMIC ROBUSTNESS OF REACTOR TRIP VIA CONTROL ROD INSERTION AT INCREASED SEISMIC HAZARD ESTIMATES

Manuel Pellissetti<sup>1</sup>, Andrii Nykyforchyn<sup>2</sup>, Peter Rangelow<sup>1</sup>, Konrad Schramm<sup>1</sup>, Hannes Keßler<sup>1</sup>, Jens-Uwe Klügel<sup>2</sup>, Ulrich Klapp<sup>1</sup>

<sup>1</sup> AREVA GmbH, Germany

<sup>2</sup> Kernkraftwerk Gösgen-Däniken, Switzerland

### ABSTRACT

A comprehensive seismic safety demonstration of the reactor trip for the 3-loop PWR (pressure water reactor) at the Gösgen NPP (nuclear power plant) is presented. The demonstration addresses an increased seismic hazard estimation resulting from the probabilistic seismic hazard analysis for Swiss NPP sites (PEGASOS).

The analysis focusses on the following relevant failure modes:

- (i) excessive inelastic deformation of the fuel assemblies due to spacer grid buckling,
- (ii) excessive deformation of the control rod pressure tubes,
- (iii) excessive relative displacement between RPV (reactor pressure vessel) internals, and
- (iv) damage of the RPV internals and the CRDMs (control rod drive mechanisms).

A staggered approach has been followed in the evaluation of the robustness. In a first step, the robustness of the reactor trip has been evaluated based on existing design documents, resulting in an estimate of the HCLPF (High Confidence of Low Probability of Failure) capacity based on the CDFM (conservative deterministic failure margin) method.

The second step involved a full scope probabilistic dynamic reanalysis of the entire analysis chain, consisting of a SASSI-model of the reactor building, an ANSYS-model of the RPV including the internals, fuel assemblies and CRDMs, and a dedicated impact model of the fuel assemblies using the proprietary simulation code KWUSTOSS. Based on this reanalysis, fragility curves were developed using the separation of variables method.

The main conclusions of the study consist in

- (i) validation of the conservative CDFM-based HCLPF capacities via a fully featured, Latin Hypercube Sampling based probabilistic dynamic analysis, and
- (ii) quantitative evidence that inelastic deformation of the spacer grids implies significantly reduced response variabilities in the corresponding fragility analysis.

### INTRODUCTION

In 2001 an extensive re-assessment of the seismic hazard to be considered at Swiss NPP sites was started under the acronym PEGASOS (“Probabilistische Erdbebengefährdungsanalyse für die KKW-Standorte in der Schweiz”). The preliminary ground motion parameters released for the individual sites so far, are significantly higher than those considered at the time of licensing. Swiss NPP operators are required to demonstrate that systems, structures and components required for bringing and maintaining the plant in a safe shutdown state do not suffer unacceptable degradation in case of seismic ground motion corresponding to a mean exceedance frequency of  $10^{-4}$  per year (“review-level-earthquake”→RLE). This can be accomplished by demonstrating that the HCLPF capacity is equal to or higher than the PGA (peak ground acceleration) of the RLE; refer to the section “HCLPF estimation based on CDFM” for the definition of the HCLPF capacity.

Within this context, the present paper describes quantitative studies regarding the seismic robustness of the reactor trip at the Gösgen NPP, a three-loop PWR (1035 MWe) on the Aare river, in operation

since 1979. It is noted that the results of these quantitative studies are based on preliminary hazard data – as mentioned in the previous paragraph - and are thus to be considered as preliminary.

As illustrated in the left portion of Figure 1, several potential failure modes may prevent the control rods from reaching the position of full insertion within the required time window.

The failure modes are classified as follows:

- Excessive deformation of the control rod drive mechanism (CRDM, bullet 1 in the left portion of Figure 1 below)
- Excessive relative displacements of the reactor pressure vessel internals (bullets 2 and 3), either due to slippage between sub-components or damage to highly stressed parts
- Excessive fuel assembly deformation (bullet 4)

In accordance with the regulatory requirements in Switzerland, the selected trial RLE consists in the mean UHS (uniform hazard spectra) for an exceedance frequency of  $10^{-4}$  per year, i.e. by the red lines in the right portion of Figure 1 below. The solid line denotes the horizontal component and the dashed line denotes the vertical component of the spectral acceleration.

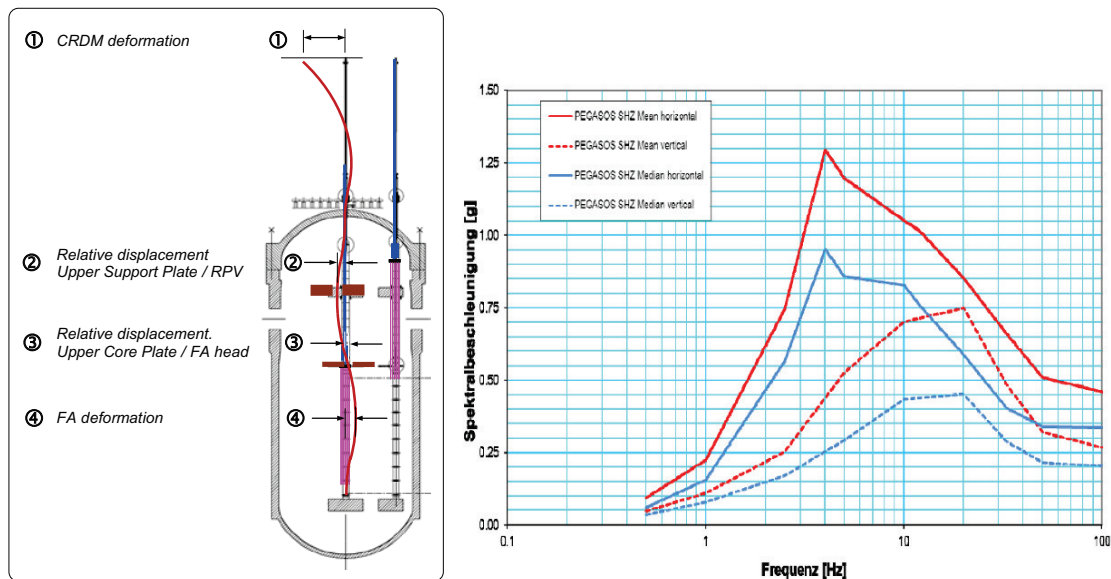


Figure 1. Analyzed failure modes (left) and preliminary mean and median UHS (5% damping) at the free field surface for an exceedance frequency of  $10^{-4}$  per year (right)

The quantitative studies of the HCLPF capacity of the reactor trip are conducted using two distinct approaches – to be described later –, namely i.) CDFM and ii.) fragility analysis by separation-of-variables. Both approaches make use of probabilistic floor responses which will thus be described next.

## PROBABILISTIC FLOOR TIME HISTORIES AND RESPONSE SPECTRA

### *Civil Structures*

The reactor building of the three-loop PWR at Gösgen is shown on the left of Figure 2 below. The dynamic analysis is performed with SASSI, using the beam model shown on the right of Figure 2. The soil structure interaction model accounts for partial embedment and for ground motion incoherence. The latter is modeled by two different models: in the first stage (HCLPF estimation by CDFM), filter functions according to FEMA (2005) are used, whereas in the second stage (fragility analysis) filter functions according to Abrahamson (2006) are used.

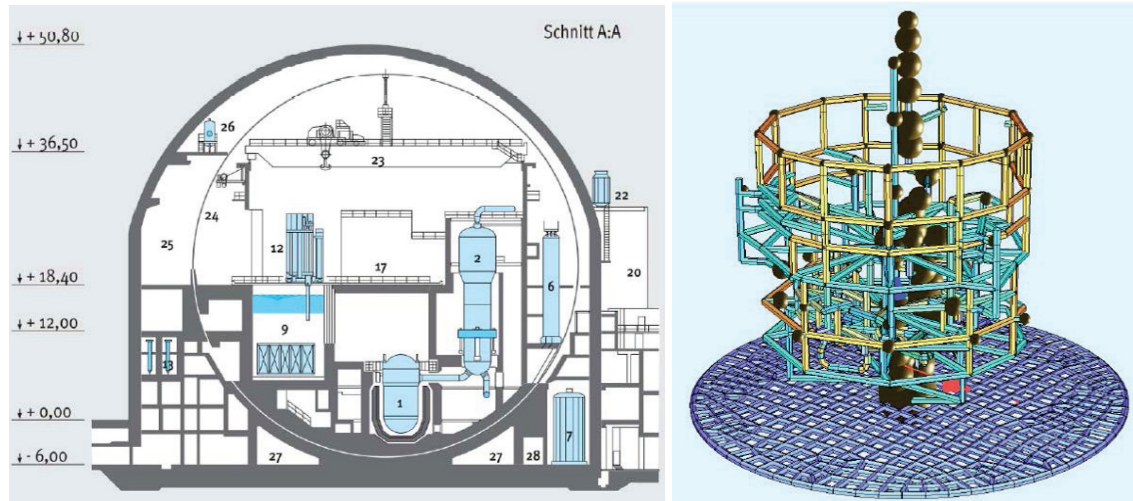


Figure 2. Reactor building – section (left) and beam model with rigid foundation slab (right)

### ***Probabilistic modeling***

The variability in the following parameters was modeled:

1. Ratio between the zero-period acceleration (ZPA) of the two horizontal acceleration components
2. Angle of orientation of the two horizontal acceleration components, with respect to the site specific coordinate system
3. Dynamic shear modulus  $G$  of the soil
4. Damping ratio  $D$  of the soil
5. Young's modulus  $E$  of the reinforced concrete reactor building structures
6. Damping ratio  $D$  of the reinforced concrete reactor building structures
7. Incoherence

The first two parameters represent aleatory variability associated with the seismic ground motion, whereas parameters three through seven represent epistemic uncertainty with respect to the modeling of the structures.

The type and magnitude of the assumed variability is summarized in the following Table 1.

Table 1: Probabilistic modeling of variability in reactor building parameters (LN denotes lognormal)

	ZPA	Angle	G-Soil	D-Soil	E-Structure	D-Structure	Incoherence*
Distribution	uniform	uniform	LN	LN	LN	LN	LN
Variability	[1.0; 1.6]	[0°; 360°]	0.5	0.35	0.5	0.35	0.1

The asterisk next to “Incoherence” indicates that this variability model is applied only in the first stage of the study (HCLPF estimation by CDFM), in combination with the incoherence model according to FEMA (2005). The incoherence model used in the second stage implicitly includes the variability; no additional variability needs thus to be introduced.

For the above listed parameters a random sample of size 30 is generated using the Latin-Hypercube sampling scheme.

### ***Dynamic analysis***

In correspondence with the parameter sampling described in the previous subsection, a set of 30 artificial ground motion time histories is generated, matching the median PEGASOS  $10^{-4}/a$  UHS, shown by the blue curves in the right portion of Figure 1. The ZPA of the horizontal component corresponds to 0.337 g, the vertical one to 0.204 g.

Using these ground motion time histories, the probabilistic floor response spectra (median and 84% fractiles) are generated with the model shown in Figure 2. The output node of interest, for which three displacements and three rotations are output, is chosen at the location of the RPV support.

The probabilistic floor response spectra are used for the HCLPF estimation based on CDFM (stage 1), whereas the sample of time histories is used for the fragility analysis via separation of variables (stage 2).

### **HCLPF ESTIMATION BASED ON CDFM (STAGE 1)**

#### ***Definition of the HCLPF capacity***

The HCLPF capacity is defined as the value of the PGA for which there is a high confidence (95%) that the probability of failure does not exceed 5% (the acronym HCLPF stands for “High Confidence of Low Probability of Failure”).

#### ***CDFM method***

The CDFM method is described in Appendix A of EPRI (2009).

In a first step, the RLE is to be defined; note that in EPRI (2009) is termed SME (seismic margin earthquake). In the present study, the RLE consists in mean PEGASOS  $10^{-4}/a$  UHS (red curves in the right portion of Figure 1).

The elastic seismic demand induced by the RLE is then to be conservatively quantified; in quantitative terms, the demand is to be quantified at a probability of non-exceedance of 84%.

Based on these definitions, the HCLPF capacity can be estimated to be equal to the RLE, if the following inequality holds:

$$\frac{\text{Elastic seismic demand}}{\text{Strength}} \leq F_N \quad (1)$$

where the respective code allowable can be used for the strength and  $F_N$  represents the inelastic energy absorption factor.

In the present study, the above stated criteria related to the conservative quantification of the seismic demand is satisfied by using the 84% fractile of the probabilistic floor response spectra described in the previous section.

#### ***Fuel assembly modelling***

The fuel assemblies in the core are represented by a 2D-model (left portion of Figure 3 below), in order to study the dynamic response in the time domain with the proprietary software code KWUSTOSS. The fuel assemblies are modelled by linear beams coupled at the top and at the bottom to the motions of the grid plate and the lower core plate, respectively. The reduction of the lateral fuel assembly stiffness over its lifetime, due to irradiation, is taken into account by considering several core configurations with both beginning-of-life and end-of-life fuel assembly stiffness properties.

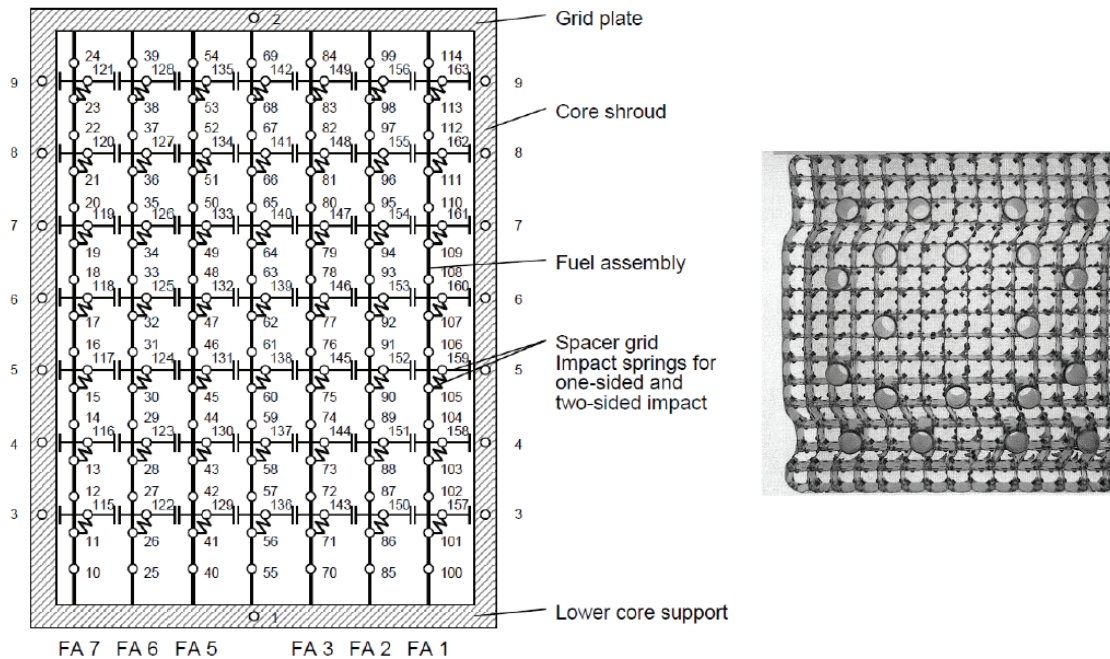


Figure 3. Fuel assembly model (left) and buckled spacer grid after compression test (right)

Adjacent fuel assembly beams interact with each other at the spacer grid levels via nonlinear elastoplastic impact couplings between the spacer grid impact nodes attached to the beams. Impacts between the moving core shroud and the fuel assemblies at the core boundary are modelled in a similar way. The idealized elastoplastic force-deflection characteristics of the impact couplings are determined from compression tests with two-sided, one-directional loading of the spacer grids (right portion of Figure 3). Irradiation of the spacer grids in reactor conditions leads to partial loss of the stabilizing effect of the fuel rods on the spacer grid impact strength. Therefore, the spacer grid impact strength in the end-of-life state is used conservatively throughout all analyses.

Both two-sided and one-sided impacts are considered. During two-sided impacts the impact loads are exclusively resisted by the in-plane stiffness of the spacer grid. Impact loads due to one-sided impacts are resisted both by the in-plane stiffness of the spacer grid and the local bending stiffness of the fuel assembly. More specifically, relative motions between the fuel assembly skeleton (consisting of the guide tubes and the spacer grids) and the fuel rods during one-sided impacts are considered in the model by linear springs connecting the spacer grid impact nodes with the corresponding beam nodes at the spacer grid levels.

Modal mass and stiffness damping of the fuel assemblies as well as nonlinear damping due to transverse fuel assembly motions in the coolant are taken into account. Linear damping of the fuel assembly motions caused by axial coolant flow is considered conservatively for the reduced flow velocity at the end of the excitation period.

The distribution of the fuel assembly types and their irradiation states in the core imply a spatial distribution of the fuel assembly stiffness and impact properties. These mixed core effects are treated in a generic way by analysing all possible combinations of one fuel assembly type in one limiting irradiation state begin-of-life or end-of-life on the control assembly positions surrounded by another fuel assembly type in one of the limiting irradiation states on the non-control assembly positions.

#### ***HCLPF capacity of the fuel assembly spacer grids***

The fuel assembly model described in the previous subsection is used for the estimation of the HCLPF capacity of the fuel assembly spacer grid (failure mode 4 in the left portion of Figure 1).



Due to the highly non-linear characteristics of the fuel assembly model, a limit analysis was performed by scaling the original design acceleration time histories representing the excitation of the fuel model, i.e. the time histories of the lower core support, the core shroud and the grid plate. The scaling factor is incremented in steps of 0.1 until a maximum permanent spacer grid deformation of 4 mm in one of the spacer grids is reached. This deformation limit is based on drop tests with fuel assemblies with perturbed geometry, showing that constraints regarding the time until full insertion are still met under these conditions, taking also into account C- and S-type bowing of the fuel assemblies under compression.

The HCLPF capacity was then estimated by comparing – at the fundamental frequency of the fuel assemblies - the scaled design floor response spectra with the 84% fractile of the probabilistic floor response spectra described in the previous section. The scaled design floor response spectra are the raw floor response spectra corresponding to the original design acceleration time histories, after applying the scaling factor identified by the above mentioned limit analysis.

The resulting HCLPF capacity amounts to 0.63 g PGA.

### ***HCLPF capacity of the CRDM***

For the deformation of the CRDM (failure mode 1 in the left portion of Figure 1), too, the HCLPF capacity is estimated on the basis of drop tests and a comparison of the design floor response spectra with the 84% fractile of the probabilistic floor response spectra.

The HCLPF capacity was estimated at 0.54 g PGA.

## **FRAGILITY CURVES (STAGE 2)**

### ***Reanalysis of dynamic response of RPV, RPV Internals and Control Rod Drive Mechanism (CRDM)***

The second stage of the quantitative studies presented in this paper differs from the first stage in that the probabilistic ground motion time histories corresponding to the selected trial RLE are propagated consistently across the entire analysis chain, consisting of the following links:

- a) 3D-model of the reactor building, including soil structure interaction (Figure 2)
- b) 2D-model of the RPV, the RPV internals and the CRDM (Figure 4)
- c) 2D-model of the fuel assemblies (Figure 3)

The coupled 2D-model of the RPV, the RPV internals – mainly the core support structures - and the CRDM is shown in the left portion of Figure 4 below. This beam model runs on the proprietary software code CESHOCK and includes a simplified version of the fuel assembly model, with a reduced number (five) of assemblies. The models corresponding to items b) and c) are thus partially overlapping, in order to adequately capture coupling effects between the individual sub-components in the RPV. The model shown in Figure 4 is the horizontal one. The loads due to the vertical excitations are not reanalysed via time history analysis; instead, the design loads are scaled proportionally to the increase of the vertical floor response spectra.

For selected coupling elements - such as alignment keys - detailed finite element modeling is adopted to obtain accurate representations of the force-displacement relationship (see right portion of Figure 4), which are then used in the CESHOCK model.

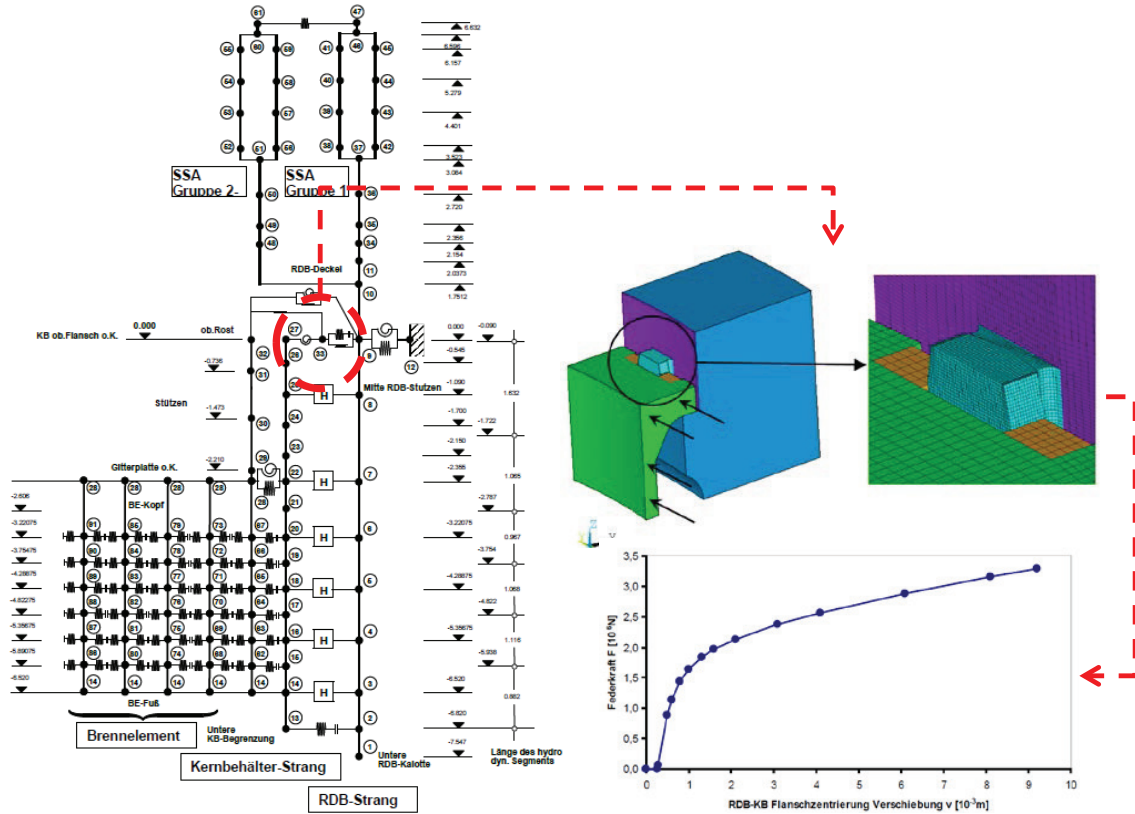


Figure 4. Dynamic analysis model for RPV, RPV internals and CRDM; global model (left) and detailed finite element modelling of local regions of interest (right)

### Fragility Curves based on Separation of Variables

The fragility model by Kennedy and Ravindra (1984), commonly used in seismic risk analysis of NPP, expresses the failure probability (“fragility”)  $F$  as a function of the level of ground motion  $a$  :

$$F(a) = \Phi \left( \frac{\ln\left(\frac{a}{\tilde{A}}\right) + \beta_U \Phi^{-1}(Q)}{\beta_R} \right) \quad (2)$$

In the above equation,  $a$  is the peak ground acceleration (PGA),  $\tilde{A}$  is the median seismic capacity (in terms of PGA),  $\beta_R$  and  $\beta_U$  are the logarithmic standard deviations due to random variability and uncertainty, respectively,  $Q$  is the confidence level and  $\Phi$  is the cumulative distribution function of the standard normal distribution. The fragility  $F$  is then the conditional failure probability, in case of a seismic event leading to a PGA equal to  $a$  .

For a given set of fragility parameters  $\tilde{A}$ ,  $\beta_R$  and  $\beta_U$ , the HCLPF capacity, introduced in an earlier section of this paper, can be directly calculated:

$$HCLPF = \tilde{A} \cdot \exp(-1.645 \cdot (\beta_R + \beta_U)) \quad (3)$$

By averaging over the uncertainty (represented by  $\beta_U$ ), one obtains the composite fragility curve:

$$F_c(a) = \Phi \left( \frac{\ln\left(\frac{a}{\bar{A}}\right)}{\beta_C} \right) \quad (4)$$

where  $\beta_C = \sqrt{\beta_R^2 + \beta_U^2}$  is the composite variability. It can be shown that the following expression is a suitable (conservative) approximation of the HCLPF value

$$HCLPF \approx \bar{A} \cdot \exp(-2.33 \cdot \beta_C) \quad (5)$$

The expression on the right is equivalent to the 1%-fractile of the capacity  $A$ . The median capacity  $\bar{A}$  in equations (2) through (5) can be expressed as

$$\bar{A} = S\bar{F} \cdot A_{\text{ref}} \quad (6)$$

where  $A_{\text{ref}}$  is the PGA of the reference ground motion (in the present case the median UHS for  $10^{-4}$  per year) and  $S\bar{F}$  may be viewed as a median safety margin factor. More specifically, it is the largest factor by which the reference ground motion can be scaled before the demand obtained with the median model lead to a violation of the failure criteria corresponding to the failure mode under consideration. The failure criteria, too, are to be defined at 50% probability of exceedance (median). For additional details it is referred to Reed and Kennedy (1994).

The main advantage of the log-normal fragility model is that it facilitates a divide-and-conquer approach. The fragility parameters  $\bar{A}$ ,  $\beta_R$  and  $\beta_U$  are thereby estimated in terms of the conservative bias and the variability introduced in the various steps of the analysis, starting from the surrounding soil, proceeding through the building, finally considering the design of the individual component (“separation-of-variables”). Each of the sources of bias and/or variability is represented by a specific factor. Depending on the position within the analysis chain, the factors are assigned to either one of the following three groups: structural response factors, equipment response factors and capacity factors. In the present study it is not necessary to evaluate the structural response factors individually, because in each realization of the sample of 30 time history analyses all variabilities related to the ground motion and the reactor building model are represented explicitly (recall the itemization of the sources of variabilities in the section “Probabilistic floor time histories and response spectra”).

### ***Fragility curves of the RPV internals and the CRDM***

As during stage 1 (HCLPF estimation by CDFM), excessive deformation of the CRDM is considered as a potential failure mode and the corresponding fragility curve is derived applying the separation-of-variables approach described in the previous subsection. In Figure 5, the corresponding composite fragility curve (equation (4)) is the green dashed curve, labelled as “Fr\_CRDM\_disp”.

In addition to the CRDM deformation, during stage 2 of the quantitative studies presented in this paper, damage of highly stressed parts of the RPV internals and of the CRDM assembly is also considered as a potentially governing failure mode for the reactor trip. More specifically, the fragility curves of the upper flange of the core barrel (CB) and of the lower part (nozzle) of the CRDM



pressure housing are developed and shown in Figure 5 below: the composite fragility curve corresponding to the core barrel upper flange is the red solid curve, labelled as “Fr\_CB\_flange”, whereas the composite fragility curve corresponding to the CRDM pressure housing is the blue dotted curve, labelled as “Fr\_CRDM\_str”.

The HCLPF capacities corresponding to the fragility curves shown in Figure 5 are compiled in the right-most column of Table 2.

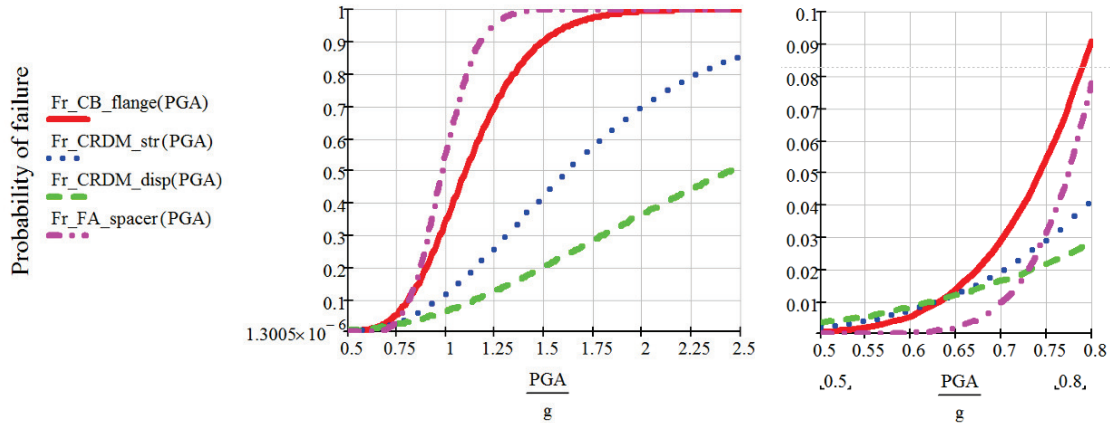


Figure 5. Composite fragility curves of analysed failure modes; full range (left) and magnification of range in which the HCLPF values are located (right)

Table 2: HCLPF capacities of failure modes relevant for reactor trip

	Stage 1 (CDFM)	Stage 2 (Fragility analysis)
Fuel assembly spacer grids (“Fr_FA_spacer”)	0.63 g	0.72 g
Deformation CRDM tubes (“Fr_CRDM_disp”)	0.54 g	0.66 g
Core barrel upper flange (“Fr_CB_flange”)	N/A	0.64 g
CRDM pressure housing (“Fr_CRDM_str”)	N/A	0.63 g

***Fragility curves of the fuel assembly spacer grids***

Finally, the fragility of the fuel assembly spacer grids is determined. As during stage 1, due to the highly non-linear phenomena governing the impact loading on the spacer grids, the largest admissible scaling factor is evaluated via limit analysis.

More specifically, an individual limit analysis is performed for each of the ten time histories leading to the highest spacer grid impact forces. This distinguishes the fragility evaluation of this failure mode from the other ones, where the seismic loads due to earthquakes stronger than the RLE are estimated by linear scaling.

Based on the variability of resulting sample of scaling factors, the median capacity and the variability parameters associated with the structural response are estimated.

In Figure 5, the corresponding composite fragility curve is the magenta dash-dotted curve, labelled as “Fr\_FA\_spacer”.

### ***Discussion of the fragility curves***

The most remarkable characteristic of the composite fragility curves in Figure 5 is that the individual median capacities (value of the PGA at which the fragility curve intersects the horizontal line corresponding to a probability of failure of 0.5) are highly different, whereas the corresponding HCLPF capacities are very similar. The latter fact is represented in the right-most column of the following Table 2, where the HCLPF capacities corresponding to the individual fragility curves are compiled. In other words, the variability associated with the individual failure modes is very different. This is especially remarkable in view of the fact that the respective variability is induced by the very same variability on the input side, i.e. the variability between the individual realizations of the floor response.

In particular, the variability associated with the failure mode “permanent spacer grid deformation” is very small, which can be observed in the left portion of Figure 5, where the range in which the magenta curve raises from 0 to 1 is very small. This is clearly due to the fact that for this failure mode a limit analysis was performed with the non-linear impact model of the core. Indeed, it was observed in the limit analysis of the ten most demanding time histories that the corresponding limit scaling factors exhibited relatively low variability. In other words, the non-linear impact model has a damping effect on the response variability.

### **CONCLUSIONS**

The main conclusion of the quantitative study presented in this paper is firstly that the CDFM-based HCLPF capacities obtained in stage 1 could be validated in stage 2 by a fragility analysis, based on a probabilistic dynamic analysis of the reactor building – using Latin Hypercube sampling with sample size 30 - and a consistent propagation of time history through the entire analysis chain.

Indeed, the CDFM-based HCLPF values are slightly lower than the fragility-based ones, like it was to be expected, since the CDFM method is – as its name suggests - meant to be conservative.

The second main conclusion of this study is that the non-linear impact model used in the limit analysis of the inelastic deformation of the spacer grids strongly reduces the corresponding response variabilities in the fragility model. Compared to other failure modes, the variability on the output side (structural response factors) is much smaller, even though the variability on the input side (floor responses) is the same. The non-linear impact model may thus be viewed as a damping mechanism for variability. This effect justifies the general expectation that significant additional margins can be demonstrated by refined modeling of the non-linear response of structures and equipment and its explicit evaluation for increasing levels of seismic excitation, up to the failure limit.

Finally, it is reiterated that the shown data are results of quantitative studies based on preliminary hazard data and are thus to be considered as preliminary.

### **REFERENCES**

- Abrahamson, N.A. (2006). *Program of Technology Innovation: Spatial Coherency Models for Soil Structure Interaction*. EPRI, Report No. 1014101. Palo Alto, CA.
- FEMA (2005). *FEMA 440 Improvement of Nonlinear Static Seismic Analysis Procedures*. Federal Emergency Management Agency, Washington DC.
- Kennedy, R. (2009). *Seismic Fragility Application Guide*. EPRI, Report No. 1019200. Palo Alto, CA.
- Kennedy, R.P. and Ravindra, M.K. (1984). “Seismic fragilities for nuclear power plant risk studies”. *Nuclear Engineering and Design*. 79, 47-68.
- Reed, J., and Kennedy, R.P. (1994). “Methodology for Developing Seismic Fragilities”. EPRI, Palo Alto, CA, Report No. TR-103959.
- SASSI (2010). “A Computer System for Analysis of Soil Structure Interaction”. University of California, Berkeley.